
Optimisation and modelling of thinning and geometric accuracy in incremental sheet forming combined with stretch forming

Rahul Jagtap and Shailendra Kumar*

Department of Mechanical Engineering,
Sardar Vallabhbhai National Institute of Technology,
Surat, 395007, India
Email: rkjagtap20@gmail.com
Email: skbudhwar@med.svnit.ac.in
*Corresponding author

Abstract: In the present experimental study incremental sheet forming is combined with stretch forming in order to obtain uniform thickness distribution, minimise thinning and to improve geometric accuracy of formed part. Preforming or stretch forming is initially done in order to obtain initial thickness distribution. Incremental sheet forming is then employed to obtain final part shape and thickness distribution. Forming time is also minimised considerably because of initial stretch forming process. The experiments are designed using central composite design (CCD) of response surface methodology. From the results, it is observed that preforming and preform tool shape have significant influence on sheet thinning. Also the combination of ISF and stretch forming processes yields in reduced thinning and uniform thickness distribution. Multi-performance optimisation using desirability function is also performed to improve thinning and geometric accuracy. Further mathematical models are developed which are in good agreement with the experimental results.

Keywords: incremental sheet forming; stretch forming; preforming; thickness distribution; thinning; accuracy.

Reference to this paper should be made as follows: Jagtap, R. and Kumar, S. (2019) 'Optimisation and modelling of thinning and geometric accuracy in incremental sheet forming combined with stretch forming', *Int. J. Materials Engineering Innovation*, Vol. 10, No. 1, pp.2–19.

Biographical notes: Rahul Jagtap received his MTech in Computer Aided Design and Manufacturing (CAD/CAM) from the S.V. National Institute of Technology, Surat, India in 2013. Currently, he is pursuing his PhD degree from the S.V. National Institute of Technology, he under the supervision of Dr. Shailendra Kumar. His research interests include sheet metal forming, computer aided design, manufacturing and engineering.

Shailendra Kumar is working as an Associate Professor in the Department of Mechanical Engineering at the S.V. National Institute of Technology, Surat, India. He has more than 17 years of teaching, research and administration experience. He has completed five research projects sponsored by various government agencies. He has published more than 130 research papers in various international and national journals as well as international and national conferences. Under his supervision, four PhD students and many MTech

students have completed their research/dissertation work. He is a life member of International Association of Engineers (IAENG), WASET, The IRED and the Indian Society of Mechanical Engineers (ISME).

1 Introduction

Incremental sheet forming (ISF) is a novel sheet metal forming technology. It has gained attention mainly because of its flexibility to form virtually any part shape on the same setup without the need of dedicated tooling such as a press tool. As the tooling requirement is minimal, the setup cost in ISF process is very small compared to conventional sheet metal forming processes. In addition to flexibility, ISF has several advantages over conventional sheet forming like increased formability, part shape changes are easily revised, small forming forces and any size of part can be formed provided the working area of machine is large enough to accommodate the part. However, some inherent drawbacks such as long processing time, uneven thickness distribution, poor surface finish and lower part accuracy limits application of ISF process in industries.

ISF is called as dieless forming process as no dedicated die is used while forming sheet metal parts. Parts to be formed are first modelled in computer aided design (CAD) software and tool path are generated using CAM software. Tool path is then fed to numerically controlled (NC) machine. Generally a hemispherical or flat ended forming tool is used to form sheet metal parts. A blank holder holds the sheet along its periphery and forming tool moves according to tool path program to form desired part shape. ISF has two major variants – single point incremental forming (SPIF) and two-point incremental forming (TPIF) process. The only difference between two variants is that there is a secondary support for blank sheet metal in form of secondary tool or partial die in TPIF, whereas there is no secondary support in SPIF process.

ISF is a layered forming process (Bahloul et al., 2014). As the name suggests, parts are formed incrementally in the ISF process. The part to be formed is divided in number of layers or slices and each slice is formed one after another until complete part is formed. The incremental nature of the process leads to local deformation, which in turn results in large elastic springback (Smith et al., 2013) due to the absence of dedicated die. The elastic springback is very large compared to springback in conventional forming processes which induces large inaccuracy in the final part shape. Also, parts with vertical walls cannot be formed using ISF process, because it obeys the sine law used in shear spinning process (Ambrogio et al., 2011). Thus there is a stern need to improve thickness distribution and improve accuracy in final part shape order to make the process industry acceptable.

Many researchers have applied research efforts to develop the ISF process. For example, Ham and Jeswiet (2008) presented a detailed literature review of SPIF process. Liu et al. (2014) and Echrif and Hrairi (2014) studied the effect of process parameters on surface roughness. Further Liu et al. (2014) optimised the process parameters using response surface methodology (RSM) to improve the surface quality. Radu and Cristea (2013) and Kurra and Regalla (2015) studied the influence of process parameters on surface finish and accuracy. Fiorentino et al. (2011) and Formisano et al. (2017)

compared negative and positive ISF process in terms of formability, sheet thinning, surface roughness and part accuracy. Authors observed that positive ISF process results in higher geometric accuracy, higher formability and lower sheet thinning. Some researchers (Young and Jeswiet 2004; Li et al., 2012, 2015) studied single pass and multi-pass forming process in order to improve thickness distribution and to reduce thinning. Considerable improvement in thickness distribution was observed and thinning was reduced. Mathematical equations were also developed to find exact number of forming stages (Li et al., 2012) and to predict the thickness (Li et al., 2015) after multi-pass forming process. Some researchers (Malhotra et al., 2011; Lingam et al., 2015; Panjwani et al., 2017) observed that geometric accuracy of parts formed is improved by using TPIF process. Excessive sheet thinning is also reduced and thickness distribution is improved using TPIF process (Malhotra et al., 2011; Moser et al., 2016). Tool path optimisation was done to improve thinning and dimensional accuracy of parts formed using ISF process (Behera et al., 2015; Azaouzi and Lebaal, 2012; Nirala and Agrawal, 2018). Forming time was reduced considerable by tool path optimisation technique (Azaouzi and Lebaal, 2012). Effect of different tool path strategies such as helical and profile tool path on thickness distribution was also studied (Jagtap et al., 2015).

This gradual improvement in the process does not seem satisfactory because of the limited application of ISF process in the industries. To make up with the limitations of conventional ISF process, some researchers have found an interesting alternative – to combine the ISF process with some other forming process or mechanism (Araghi et al., 2011). This new process is called as hybrid incremental sheet forming (HISF) process as it combines the advantages of both ISF and allied processes. For example, when a dynamic laser heating unit is used in synchronisation with ISF process, considerable improvement in geometric accuracy and formability is achieved (Duflou et al., 2007; Göttmann et al., 2011). Also, difficult-to-form materials such as titanium and magnesium alloys can be easily formed by combining ISF with electric hot forming process eliminating the need of alternate heating unit (Fan and Gao, 2014; Honarpisheh et al., 2016; Xu et al., 2016). Desired thickness distribution can be achieved by combining ISF and stretch forming (SF) process (Araghi et al., 2009; Lu et al., 2014; Tandon and Sharma, 2016). Incremental hydroforming process with reconfigurable multipoint forming tool was proposed by Liu et al. (2016) which eliminates the need of dedicated punch. Instead, a multipoint tool is used which can be used to adjust the shape of punch according to the final thickness distribution along formed part.

After extensive literature review, it has been observed that HISF comprising ISF combined with SF process is a viable option to conventional ISF process because of its ability to form parts with reduced processing time, uniform thickness distribution and reduced thinning. Till date, a handful of researchers like Araghi et al. (2009) and Lu et al. (2014) have applied research efforts to study and develop this process. Authors studied this HISF process considering only limited parameters such as preform tool shape. Extensive research effort considering more process parameters should be carried out for better understanding of the process. In depth study of these parameters will help in understanding the process mechanics and forming parts with desired accuracy and thickness distribution.

In the present experimental investigation, research efforts have been applied to investigate the effect of different process parameters like preforming (preforming depth),

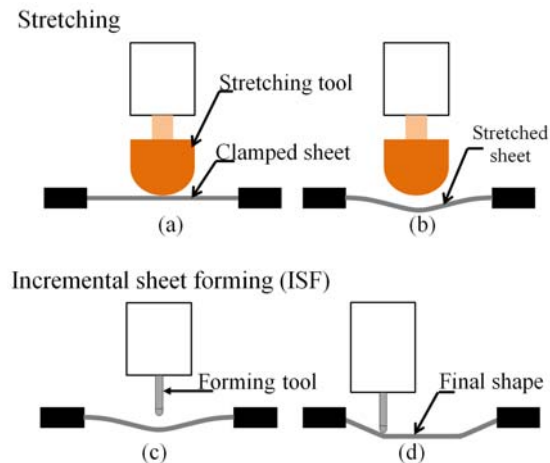
perform tool radius, ISF tool diameter and pitch. Experiments are designed using central composite design (CCD) for RSM. Multi performance optimisation using desirability function has been done to improve the performance of process.

2 Methodology

The details of experimental facility, determination of thinning and geometric accuracy and the experimental design procedure adopted for the study are described in this section.

The term ‘hybrid forming’ implies that this process is combination of two processes. In the present work, hybrid incremental forming method comprising ISF combined with SF is adopted for forming of sheet metal parts. As depicted in Figure 1(a) and Figure 1(b), preforming or SF is first done in order to get initial shape and thickness distribution. After preforming or SF, incremental forming is implemented to obtain final part shape [Figures 1(c) and 1(d)].

Figure 1 Working principle of the HISF process (incremental forming combined with SF)
(see online version for colours)



2.1 Experimental setup

Experiments are carried out on the conventional 3-axis computer numerically controlled (CNC) vertical milling machine. Aluminium alloy Al 1050-O with thickness of 1.2 mm is used as a blank sheet metal for the forming process. A frustum of cone having base diameter of 90 mm and wall angle of 50° having maximum height of 34 mm is formed. As depicted in Figure 2, fixture holds the sheet metal along its periphery and forming tool forms the part. Fixture is made of cast iron by welding L-shaped angles to form a rig which becomes the base. Two steel plates are used to hold the sheet in position. Lower plate acts as a backing plate and avoids unnecessary bending of sheet metal in the forming process. The sheet metal blank is clamped on the fixture using nut and bolts. Preforming tools used for stretching are hemispherical in shape and are made of wood as

depicted in Figure 3(a). Preforming tools are made of wood because of its lower cost and easy availability. Also it can be fabricated into desired shape very easily. Tools used for ISF process are made of stainless steel SS-304 [Figure 3(b)]. The radius of preforming tool ranges from 50 mm to 90 mm while radius of ISF tools ranges from 3 mm to 7 mm.

Figure 2 Fixture used for HISF process (see online version for colours)

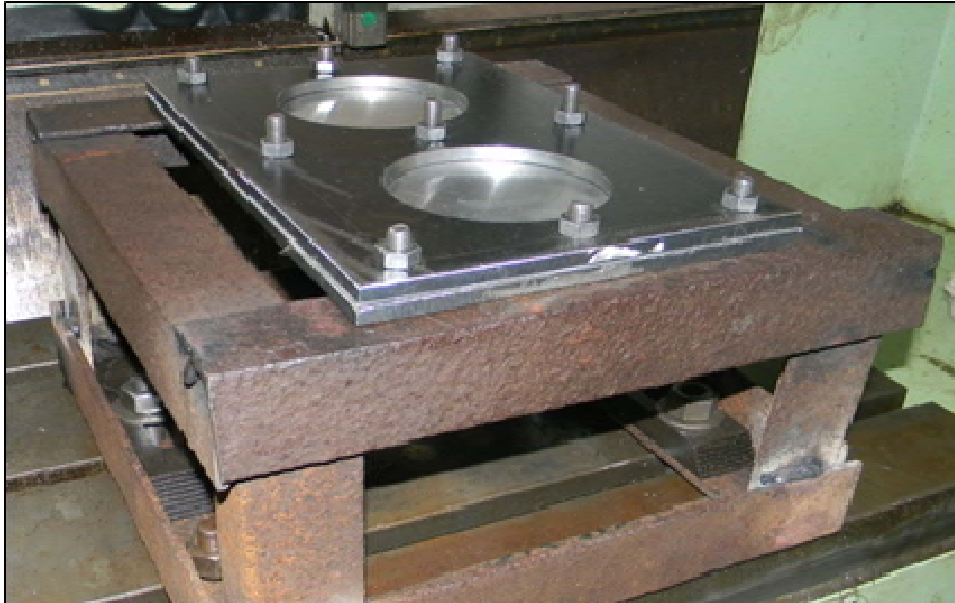


Figure 3 Preforming or SF tool (wooden) and ISF tools (ss-304) (see online version for colours)



(a)

(b)

Table 1 Forming parameters and levels

<i>Parameters</i>	<i>Symbols</i>	<i>Levels</i>				
		<i>-2</i>	<i>-1</i>	<i>0</i>	<i>1</i>	<i>2</i>
Preforming (mm)	A	10	12	14	16	18
P_rad (mm)	B	50	60	70	80	90
T_dia (mm)	C	6	8	10	12	14
Pitch (mm)	D	0.2	0.4	0.6	0.8	1.0

Table 2 RSM deign matrix used for experimentation

<i>Standard</i>	<i>Run</i>	<i>Preforming</i>	<i>P_rad</i>	<i>T_dia</i>	<i>Pitch</i>
1	1	-1	-1	-1	-1
2	28	1	-1	-1	-1
3	15	-1	1	-1	-1
4	27	1	1	-1	-1
5	9	-1	-1	1	-1
6	2	1	-1	1	-1
7	25	-1	1	1	-1
8	18	1	1	1	-1
9	6	-1	-1	-1	1
10	5	1	-1	-1	1
11	7	-1	1	-1	1
12	22	1	1	-1	1
13	16	-1	-1	1	1
14	20	1	-1	1	1
15	23	-1	1	1	1
16	13	1	1	1	1
17	29	-2	0	0	0
18	4	2	0	0	0
19	30	0	-2	0	0
20	11	0	2	0	0
21	8	0	0	-2	0
22	12	0	0	2	0
23	14	0	0	0	-2
24	10	0	0	0	2
25	24	0	0	0	0
26	19	0	0	0	0
27	21	0	0	0	0
28	17	0	0	0	0
29	26	0	0	0	0
30	3	0	0	0	0

Experiments are designed according to CCD for RSM. Total 30 experiments are carried out according to the RSM design plan. Table 1 presents the process parameters with their levels and Table 2 presents the design matrix used for the experimentation purpose. Effect of four process parameters namely preforming (depth of stretching), preforming tool radius (P_{rad}), ISF tool diameter (T_{dia}) and pitch (vertical step depth) on responses namely minimum thickness (T) and geometric accuracy in terms of root mean square error (RMSE) is studied.

2.2 Measurement of responses

Thickness is measured along the formed part at six different locations using standard thickness gage. Minimum thickness (T) is used as response for the statistical analysis. The response geometric accuracy is measured in terms of RMSE. Formed cones are trimmed along its periphery using abrasive water jet machine (AWJM) to avoid unwanted bending. After trimming, formed parts are masked with white colour from outside and scanned using a laser scanner. The masking makes it easy for the laser scanner to scan objects accurately. The scanned part data is stored in the form of point cloud data. The point cloud data is then extracted in SolidWorks 2012. Using this point cloud data, outer profile of the formed part is generated. This profile is compared with standard part profile geometry. The difference in target part geometry and formed part geometry is measured at 41 different points. The geometric error is then converted to RMSE using equation (1):

$$RMSE = \sqrt{\frac{\sum_{i=1}^n (x_i - x_o)^2}{n}} \quad (1)$$

where

x_i target values

x_o observed value.

3 Analysis of results

This section provides experimental results of thinning and geometric accuracy according to CCD design. Effect of process parameters on the responses is discussed in details followed by the optimisation of two responses using desirability function.

The CCD for RSM was applied using Design Expert software based on selected process parameters and their levels as listed in Table 1. Four process parameters were selected for the experimental purpose and each parameter was varied at five levels. Experiments are conducted in the sequence specified by the CCD design. ANOVA is performed to identify significance and influence of selected process parameters on the responses. The present analysis is carried out at confidence level of 95%. In this analysis mathematical models are fitted according to surfaces presented by independent variables. According to experimental analysis, second order quadratic equations are developed to represent the response surface that fitted to the data.

The sequential F-test and lack-of-fit test are used to check adequacy of the model and ANOVA technique is used to obtain the best fit model. In ANOVA, F-value is the ratio

of model mean square to the appropriate error mean square. However, F-value becomes large if variance contributed by the model is significantly larger than the random error. Further the probability of getting observed F-value to accept null hypothesis is the probability of a larger F-value (i.e., p-value). But null hypothesis is rejected at smaller probability values. Therefore, the model terms are supposed to be significant in response if the p-value is less than 0.05.

3.1 Thinning

Table 3 lists the result of ANOVA for minimum thickness T. The model F-value of 11.9 implies the model is significant. There is only a 0.01% chance that an F-value this large could occur due to noise. Values of 'Probability > F' less than 0.05 indicate model terms are significant. In this case A, B, D, AC, BC, A², B² and C² are significant model terms. Values greater than 0.1 indicate the model terms are not significant. The lack of fit F-value of 2.18 implies there is a 19.95% chance that a lack of fit F-value this large could occur due to noise.

Table 3 ANOVA table for minimum thickness T

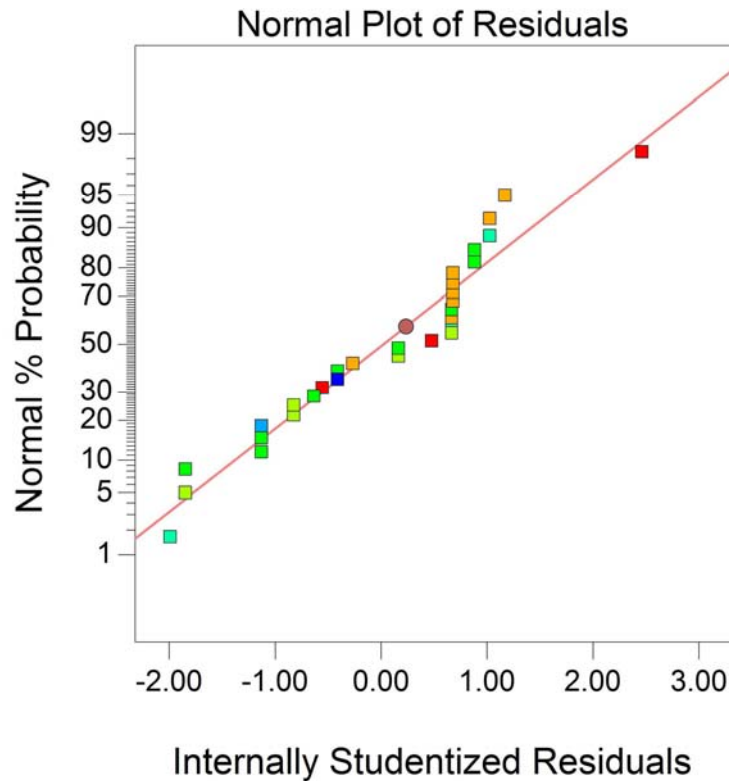
Source	Sum of squares	DF	Mean square	F value	p-value prob. > F	Remarks
Model	0.005382	9	0.000598	11.9031	< 0.0001	Significant
A-Preforming	0.001667	1	0.001667	33.1754	< 0.0001	
B-P_Rad	0.00135	1	0.00135	26.872	< 0.0001	
C-T_Dia	0.00015	1	0.00015	2.9858	0.0994	
D-Pitch	0.000817	1	0.000817	16.2559	0.0007	
AC	0.0004	1	0.0004	7.9621	0.0105	
BC	0.000225	1	0.000225	4.4787	0.0471	
A ²	0.000322	1	0.000322	6.4159	0.0198	
B ²	0.000322	1	0.000322	6.4159	0.0198	
C ²	0.000322	1	0.000322	6.4159	0.0198	
Residual	0.001005	20	5.02E-05			
Lack of fit	0.000871	15	5.81E-05	2.1786	0.1995	Not significant
Pure error	0.000133	5	2.67E-05			
Cor. total	0.006387	29				

Minimum thickness (T) observed is in the range of 0.68 mm to 0.74 mm. According to analysis, final regression equation for minimum thickness (T) in terms of coded is given in equation (2):

$$\begin{aligned}
 T = & 0.73 - 8.33 \times 10^{-1} A + 7.5 \times 10^{-3} B \\
 & - 2.5 \times 10^{-3} C - 5.83 \times 10^{-3} D \\
 & - 5 \times 10^{-3} AC + 3.75 \times 10^{-3} BC \\
 & - 3.39 \times 10^{-3} A^2 - 3.39 \times 10^{-3} B^2 \\
 & - 3.39 \times 10^{-3} C^2
 \end{aligned} \tag{2}$$

As depicted in normal probability plot (Figure 4), the data follows a normal distribution as all the data points are following a straight line. The adj. R^2 of 0.8427 is in reasonable agreement with R^2 of 0.7719.

Figure 4 Normal probability plot (see online version for colours)



Thickness distribution is a function of preform shape (Martins et al., 2013). As the preforming radius increases from 60 mm to 80 mm, thickness increases as depicted in Figure 5. The increase in thickness occurs because while preforming or stretching a part with larger diameter tool increases the area of contact between tool and sheet. Therefore the strain distribution while stretching is spread over a larger surface area for the given preforming depth. In case of smaller preforming tool radius, the contact area between tool and sheet is small. Therefore localised thinning takes place further reducing the thickness.

From Figure 5, it can be observed that as preforming increases from 12 mm to 16 mm, minimum thickness decreases or thinning increases. This happens because preforming results in plastic deformation, resulting in thickness reduction. After preforming process, ISF process further reduces the thickness resulting in more thinning. As discussed earlier, thickness distribution is a function of the preform shape. Therefore the combined effect of preforming shape and preforming depth should be considered in order to improve thinning in parts formed using incremental forming combined with SF process.

Figure 5 Effect of P_rad and preforming on minimum T (see online version for colours)

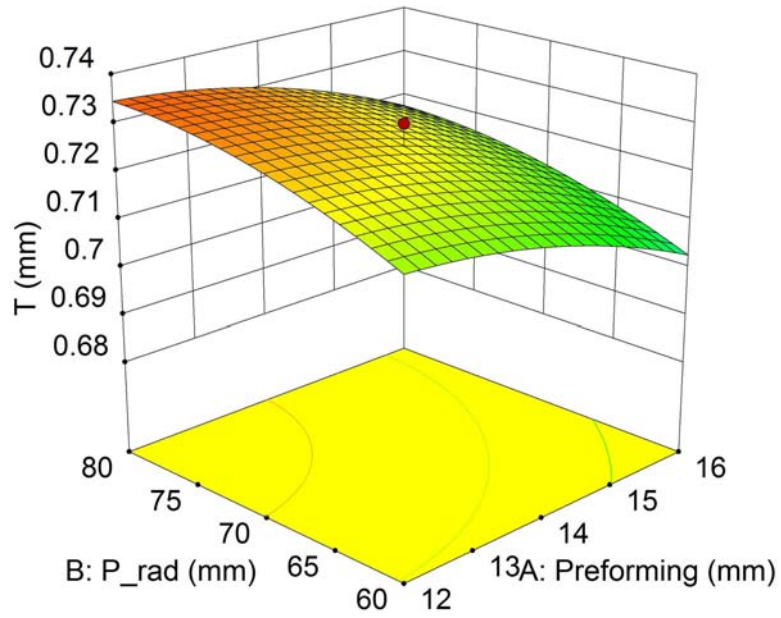


Figure 6 Effect of T_dia and preforming on minimum T (see online version for colours)

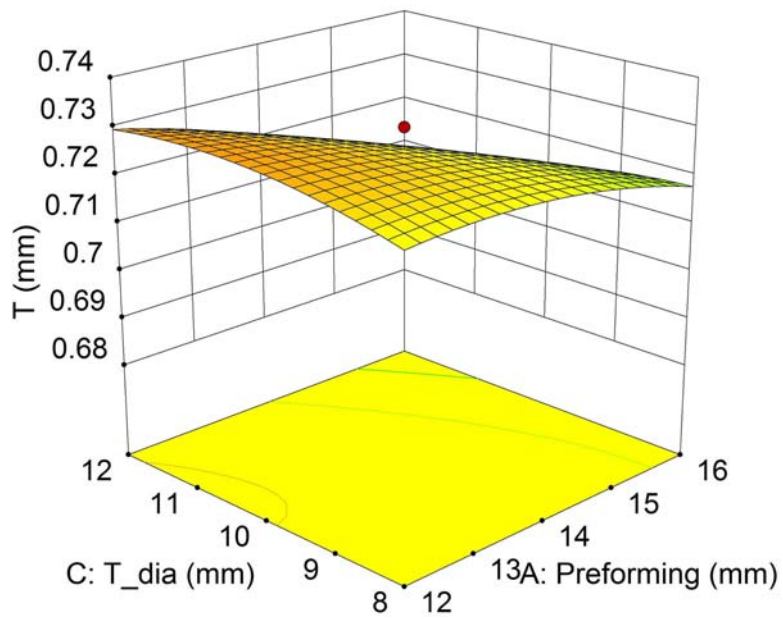
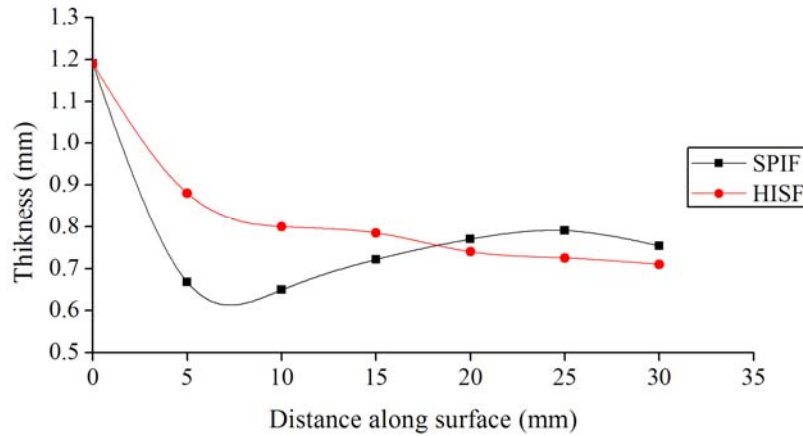


Figure 7 Thickness profile for cone formed by SPIF and HISF process (see online version for colours)

Size of ISF forming tool (T_{dia}) has small effect on the thinning in the forming process. As depicted in Figure 6, it can be observed that as the tool diameter increases, thickness also increases. For a given pitch or step depth, as the tool diameter increases, contact area between the tool and sheet also increases. When the tool moves to form next layer, because of large tool size, the tool uniformly deforms the material from same contact area, resulting in more uniform thickness distribution and reduced thinning. As tool diameter decreases, the contact area also decreases resulting in less uniform thickness distribution and more thinning.

As reported by Young and Jeswiet (2004), more thinning takes place in SPIF mainly at two locations, first near the periphery where the sheet is clamped. At this location first bending takes place followed by shear forming process. At this transition phase more amount of thinning takes place compared to thinning at other locations. Figure 7 depicts the thickness profiles for SPIF and HISF processes. It can be observed from the figure that there is a considerable improvement in thinning while forming parts with HISF. In HISF process, thinning near the clamped periphery is not observed because of initial preforming process. The plastic deformation due to the preforming process prevents initial thinning of sheet.

3.2 Geometric accuracy

A similar analysis procedure used for thinning was performed for geometric accuracy. Table 4 lists the ANOVA result for geometric error. From table 4, it can be observed that the model F-value is 30.38 which imply that the model is significant. There is only a 0.01% chance that a “Model F-value” this large could occur due to noise. Values of ‘prob. > F’ (p-value) less than 0.05 indicate model terms are significant. In this case only C, i.e., ISF tool diameter is the only significant model term. Preforming is having small influence on the geometric accuracy of parts formed by ISF process. P-values greater than 0.1 indicate the model terms are not significant. The ‘lack of fit F-value’ of 3.16 implies the lack of Fit is not significant relative to the pure error. There is a 10.25% chance that a ‘lack of fit F-value’ this large could occur due to noise. Non-significant lack of fit is good.

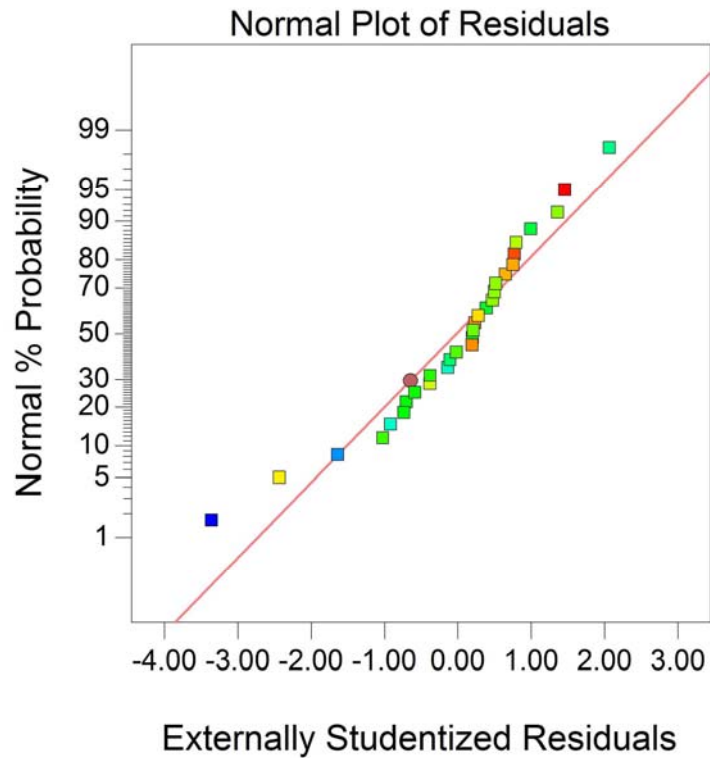
Table 4 ANOVA table for part accuracy in terms of RMSE

Source	Sum of squares	DF	Mean square	F value	p-value prob. > F	Remarks
Model	8.12	2	4.06	30.38	< 0.0001	Significant
A-Preforming	0.33	1	0.33	3.15	0.0871	
C-T_Dia	7.78	1	7.78	73.45	< 0.0001	
Residual	2.86	27	0.11			
Lack of fit	2.67	22	0.12	3.16	0.1025	Not significant
Pure error	0.19	5	0.038			
Cor. total	10.98	29				

Geometric error in terms of RMSE observed is in the range of 1.284 mm to 3.97 mm. According to the analysis, final regression equation for geometric error in terms of RMSE in coded is given in equation (3):

$$RMSE = 2.85 - 0.12A + 0.57C \tag{3}$$

Figure 8 Normal probability plot for RMSE (see online version for colours)



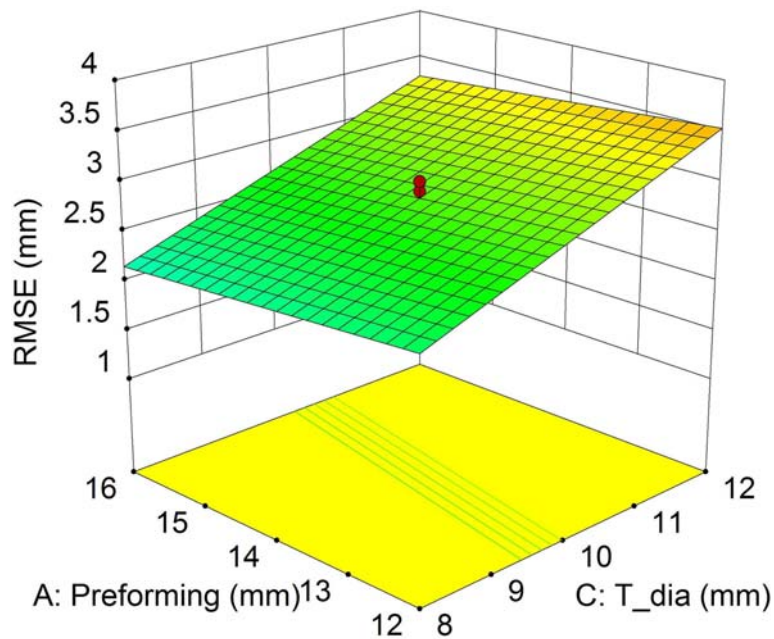
As depicted in normal probability plot (Figure 8) the data follows a normal distribution as all the data points are following a straight line. The adj. R^2 of 0.7201 is in reasonable agreement with R^2 of 0.7394

Figure 9 depicts the effect of preforming and ISF tool size on the RMSE. From the figure it can be observed that preforming has very small effect on RMSE. Preforming is used for initial thickness distribution and the final part shape is very different from the preform shape. Therefore it does not affect the part accuracy considerably.

ISF tool diameter has a considerable effect on the part accuracy. While forming parts using smaller diameter tools, the contact area between the tool and sheet is small. As the tool diameter increases, the contact area also increases. For a given pitch or vertical step depth in ISF process, tool with smaller diameter results in large plastic deformation and small elastic deformation, whereas tool with larger diameter results in considerably small plastic deformation and larger elastic deformation. Therefore the elastic recovery is small for smaller tool compared to larger tool. From figure 9 it can be observed that as tool diameter (T_dia) increases, RMSE also increases. Previous experimental results by Radu et al. (2013) show similar trends of accuracy with respect to tool size.

Another reason for this large amount of error in part accuracy is the springback in ISF process. As very large area in ISF process is unconstrained. The unconstrained sheet results in more elastic deformation compared to total plastic deformation, resulting in poor geometric accuracy in final part shape formed by SPIF process. In TPIF process, as the constraints on the sheet increases, more accurate part can be formed compared to SPIF process.

Figure 9 Effect of preforming and T_dia on part accuracy (RMSE) (see online version for colours)



4 Multi-performance optimisation

Optimisation of the process parameters is done in order to maximise thickness and to minimise the profile error, i.e., RMSE. Desirability function is used for the multi-response optimisation. It is used when the quality of product or process having different features is not acceptable if any one of them is not in the desirability limit. Its aim is to find parameter levels that fulfils the criteria of all the responses and also provides the best values of the combined response (Candiotti et al., 2014). In this approach multiple responses are converted into a dimensionless quantity of performance called as overall desirability function, $df = (d_1 \cdot d_2 \cdot d_3 \dots \cdot d_m)^{(1/m)}$ where m represents number of responses (Montgomery, 2012). Desirability is bounded by $0 \leq df \leq 1$, i.e., its scale falls from $df = 0$ to $df = 1$, where $df = 0$ is most undesirable and $df = 1$ being most desirable response.

The optimisation criteria for input parameters and responses are listed in Table 5 and Table 6. As thickness is to be maximised in order to reduce thinning, optimisation criteria for thickness is set to maximisation. RMSE is profile error or inaccuracy in final part shape. Objective of the optimisation is to minimise the profile error or improve the geometric accuracy of the formed part. Therefore criterion of optimisation for RSME is set to minimisation. Also optimisation is done at equal weightage for both the responses.

Table 5 Optimisation criteria for input parameters

Parameter	Goal	Lower limit	Upper limit
Preforming	In range	10	18
P_Rad	In range	50	90
T_Dia	In range	6	14
Pitch	In range	0.2	1.0

Table 6 Optimisation criteria for responses

Name	Goal	Lower limit	Upper limit	Lower weight	Upper weight	Importance
T	Maximise	0.68	0.74	1	1	Equal
RMSE	Minimise	1.284	3.97	1	1	Equal

Table 7 Conformation tests

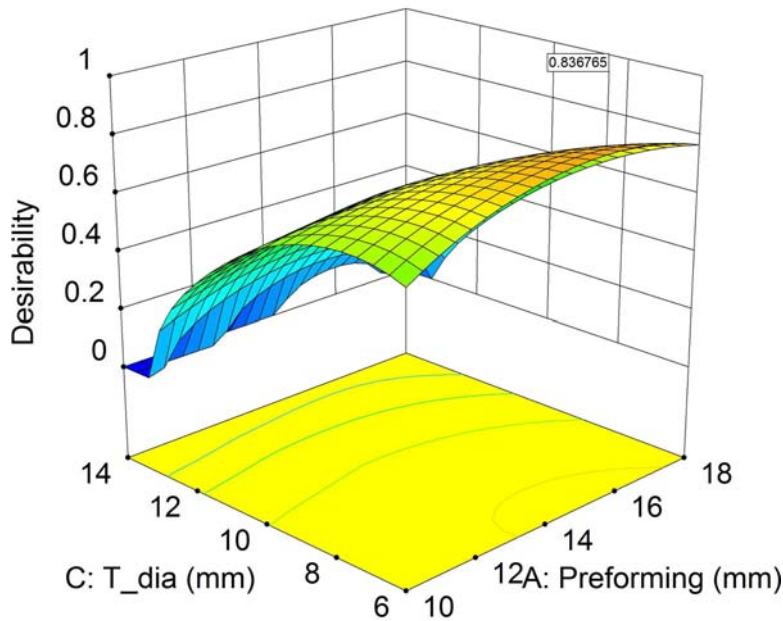
Preforming (mm)	P_rad (mm)	T_dia (mm)	Pitch (mm)	Min T (mm)		RMSE (mm)	
				Observed	Predicted	Observed	Predicted
15	90	8	0.8	0.68	0.709	2.369	2.2169
15	70	6	0.2	0.71	0.727	1.464	1.6357
14	80	10	1	0.65	0.717	2.391	2.84528
16	60	12	0.8	0.68	0.681	2.274	3.29672

Figure 10 shows the combined desirability with respect to preforming and tool diameter. It can be observed from the figure that the optimum desirability for the given set of process parameters is 0.8367 which is acceptable as it is close to 1.

Figure 10 shows the influence of T_dia and preforming on overall desirability. There is a very small influence of preforming on desirability. As preforming increases up to 15 mm, desirability increases and then starts decreasing. From the optimisation results it can be observed that optimum thickness is achieved at 15 mm preforming. T_dia is having large effect on the desirability, because part accuracy is greatly affected by tool diameter. While using smaller tool diameter for forming parts, very good part accuracy can be achieved. As the tool diameter increase, accuracy also decreases, resulting in considerable loss in the overall desirability.

Conformation tests have been conducted to verify adequacy of developed mathematical model. Random levels of each parameter are selected to carry out the confirmation tests within the given range of selected process parameters. Conformation test results are listed in Table 7. The conformation tests verify that the model prediction results are in good agreement with experimental results.

Figure 10 Effect of T_dia and preforming on overall desirability (see online version for colours)



5 Conclusions

In the present experimental work, efforts have been applied to study the influence of process parameters on thinning and thickness distribution. From the present study, the following conclusions are drawn:

- 1 There is a considerable influence of preform tool shape and preforming on the thickness distribution and thinning. As the preform shape changes, thickness distribution also changes. Optimisation of process parameters result in less thinning and improved thickness distribution.

- 2 Accuracy of the part formed depends on tool diameter (T_{dia}). Tools of smaller diameter result in forming accurate part shapes as compared to tools of larger diameter.
- 3 About 20% reduction in forming time is observed while using ISF combined with SF process.

A multi-performance optimisation using desirability function has also been performed in order to improve the thinning and geometric accuracy of formed parts. The optimum set of process parameters results in forming accurate part shape with minimum thinning as well as uniform thickness distribution. Mathematical models for thinning and geometric accuracy have also been developed which are in good agreement with experimental results. Values predicted by mathematical models results in forming parts with minimum thinning and uniform thickness distribution are achieved. Considerable improvement in the part accuracy is also achieved.

The present experimental study is beneficial for many sheet metal industries engaged in manufacturing of high-end applications such as aerospace industries, automotive industries and biomedical industries

References

- Ambrogio, G., Filice, L., Gaudio, M. and Manco, L. (2011) 'Optimised tool-path design to reduce thinning in ISF process', *International Journal of Material Forming*, Vol. 3 No. 1, pp.959–962.
- Araghi, B.T., Gottmann, A., Bambach, M., Hirt, G., Bergweiler, G., Dietrich, J., Steiners, M. and Saeed-Akbari, A. (2011) 'Review on the development of a hybrid incremental sheet forming system for small batch sizes and individualized production', *Production Engineering*, Vol. 5, No. 4, pp.393–404.
- Araghi, B.T., Manco, G.L., Bambach, M. and Hirt, G. (2009) 'Investigation into a new hybrid forming process: Incremental sheet forming combined with stretch forming', *CIRP Annals – Manufacturing Technology*, Vol. 58, No. 1, pp.225–228.
- Azaouzi, M. and Lebaal, N. (2012) 'Tool path optimization for single point incremental sheet forming using response surface method', *Simulation Modelling Practice and Theory*, Vol. 24, No. 1, pp.49–58.
- Bahloul, R., Arfa, H. and BelHadjSalah, H. (2014) 'A study on optimal design of process parameters in single point incremental forming of sheet metal by combining Box-Behnken design of experiments, response surface methods and genetic algorithms', *The International Journal of Advanced Manufacturing Technology*, Vol. 74, Nos. 1–4, pp.163–185.
- Behera, A.K., Lauwers, B. and Duflou, J.R. (2015) 'Tool path generation for single point incremental forming using intelligent sequencing and multi-step mesh morphing techniques', *International Journal of Material Forming*, Vol. 8, No. 4, pp.517–532.
- Candiotti, L.V. et al. (2014) 'Experimental design and multiple response optimization, using the desirability function in analytical methods development', *Talanta*, Vol. 124, No. 1, pp.123–138.
- Duflou, J.R., Callebaut, B., Verbert, J. and Baerdemaeker, H. (2007) 'Laser assisted incremental forming: formability and accuracy improvement', *CIRP Annals – Manufacturing Technology*, Vol. 56, No. 1, pp.273–276.
- Echraf, S.B.M. and Hrairi, M. (2014) 'Significant parameters for the surface roughness in incremental forming process', *Materials and Manufacturing Processes*, Vol. 29, No. 6, pp.697–703.

- Fan, G. and Gao, L. (2014) 'Mechanical property of Ti-6Al-4V sheet in one-sided electric hot incremental forming', *The International Journal of Advanced Manufacturing Technology*, Vol. 72, Nos. 5–8, pp.989–994.
- Fiorentino, A., Attanasio, A., Marzi, R., Ceretti, E. and Giardini, C. (2011) 'On forces, formability and geometrical error in metal incremental sheet forming', *Int. J. Materials and Product Technology*, Vol. 40, Nos. 3/4, pp.277–295.
- Formisano, A., Boccarusso, L., Minutolo F.C., Carrino L, Durante, M. and Langella, A. (2017) 'Negative and positive incremental forming: comparison by geometrical, experimental and fem considerations negative and positive incremental forming: comparison by geometrical, experimental and FEM considerations', *Materials and Manufacturing Processes*, Vol. 32, No. 5, pp.530–536.
- Göttmann, A., Dietrich, J., Bergweiler, G., Bambach, M., Hirt, G., Loosen P. and Poprawe, R. (2011) 'Laser-assisted asymmetric incremental sheet forming of titanium sheet metal parts', *Production Engineering*, Vol. 5, No. 3, pp.263–271.
- Ham, M. and Jeswiet, J. (2008) 'Single point incremental forming', *Int. J. Materials and Product Technology*, Vol. 32, No. 4, pp.374–387.
- Honarpisheh, M., Abdolhoseini, M.J. and Amini, S. (2016) 'Experimental and numerical investigation of the hot incremental forming of Ti-6Al-4V sheet using electrical current', *The International Journal of Advanced Manufacturing Technology*, Vol. 83, Nos. 9–12, pp.2027–2037.
- Jagtap, R., Kashid, S., Kumar, S. and Hussien H.M.A (2015) 'An experimental study on the effect of process parameters on surface roughness in single point incremental forming', *Advances in Materials and Processing Technologies*, Vol. 1, Nos. 3–4, pp.465–473.
- Kurra, S. and Regalla, S.P. (2015) 'Multi-objective optimisation of single point incremental sheet forming using Taguchi-based grey relational analysis', *Int. J. Materials Engineering Innovation*, Vol. 6, No. 1, pp.74–90.
- Li, J., Hu, J., Pan, J. and Geng, P. (2012) 'Thickness distribution and design of a multi-stage process for sheet metal incremental forming', *The International Journal of Advanced Manufacturing Technology*, Vol. 62, Nos. 9–12, pp.981–988.
- Li, J., Yang, F. and Zhou, Z. (2015) 'Thickness distribution of multi-stage incremental forming with different forming stages and angle intervals', *Journal of Central South University*, Vol. 22, No. 3, pp.842–848.
- Lingam, R., Srivastava, A. and Reddy, N.V. (2015) 'Deflection compensations for tool path to enhance accuracy during double-sided incremental forming', *Journal of Manufacturing Science and Engineering*, Vol. 138, No. 9, pp.1–8.
- Liu, W., Chen, Y., Xu, Y. and Yuan, S. (2016) 'Evaluation on dimpling and geometrical profile of curved surface shell by hydroforming with reconfigurable multipoint tool', *The International Journal of Advanced Manufacturing Technology*, Vol. 86, Nos. 5–8, pp.2175–2185.
- Liu, Z., Liu, S., Li, Y. and Meehan, P.A. (2014) 'Modeling and optimization of surface roughness in incremental sheet forming using a multi-objective function', *Materials and Manufacturing Processes*, Vol. 29, No. 7, pp.808–818.
- Lu, B., Zhang, H., Xu, D.K. and Chen, J. (2014) 'A hybrid flexible sheet forming approach towards uniform thickness distribution', *Procedia CIRP*, Vol. 18, No. 1, pp.244–249.
- Malhotra, R., Cao, J., Ren, F., Kiridena, V., Xia, Z.C. and Reddy, N.V. (2011) 'Improvement of geometric accuracy in incremental forming by using a squeezing toolpath strategy with two forming tools', *Journal of Manufacturing Science and Engineering*, Vol. 133, No. 6, p.61019.
- Martins, B., Santos, A.D. and Teixeira, P. (2013) 'A study on the influence of different variables for determination of flow stress using hydraulic bulge test', *Int. J. Materials Engineering Innovation*, Vol. 4, No. 2, pp.132–148.
- Montgomery, D.C. (2012) *Design and Analysis of Experiments*, 7th ed., Wiley, New York.

- Moser, N. et al. (2016) 'Effective forming strategy for double-sided incremental forming considering in-plane curvature and tool direction', *CIRP Annals – Manufacturing Technology*, Vol. 65, No. 1, pp.265–268.
- Nirala, H.K. and Agrawal, A. (2018) 'Fractal geometry rooted incremental toolpath for incremental sheet forming', *Journal of Manufacturing Science and Engineering*, Vol. 140, No. 2, p.021005.
- Panjwani, D. et al. (2017) 'A novel approach based on flexible supports for forming non-axisymmetric parts in SPISF', *International Journal of Advanced Manufacturing Technology*, Vol. 92, Nos. 5–8, pp.2463–2477.
- Radu, C., Tampu, C., Cristea, I. and Chirita, B. (2013) 'The effect of residual stresses on the accuracy of parts processed by SPIF', *Materials and Manufacturing Processes*, Vol. 28, No. 5, pp.572–576.
- Radu, M.C. and Cristea, I. (2013) 'Processing metal sheets by SPIF and analysis of parts quality', *Materials and Manufacturing Processes*, Vol. 28, No. 3, pp.287–293.
- Smith, J., Malhotra, R., Liu, W.K. and Cao, J. (2013) 'Deformation mechanics in single-point and accumulative double-sided incremental forming', *The International Journal of Advanced Manufacturing Technology*, Vol. 69, Nos. 5–8, pp.1185–1201.
- Tandon, P. and Sharma, O.N. (2016) 'Experimental investigation into a new hybrid-forming process: Incremental stretch drawing', *Proceedings of the Institution of Mechanical Engineers, Part B: Journal of Engineering Manufacture*, Vol. 232, No. 3, pp.475–486.
- Xu, D.K. et al. (2016) 'Enhancement of process capabilities in electrically-assisted double sided incremental forming', *Materials and Design*, Vol. 92, No. 1, pp.268–280.
- Young, D. and Jeswiet, J. (2004) 'Wall thickness variations in single-point incremental forming', *Proceedings of the Institution of Mechanical Engineers, Part B: Journal of Engineering Manufacture*, Vol. 218, No. 11, pp.1453–1459.